TURBULENT FLUID INTERFACES AND REGIONS IN AERO-OPTICS AND MIXING

Haris J. Catrakis [1], **Roberto C. Aguirre** [2], **Jennifer C. Nathman** [3], **and Philip J. Garcia** [4]
Aeronautics and Fluid Dynamics Laboratories, Mechanical and Aerospace Engineering
Henry Samueli School of Engineering, University of California, Irvine, CA 92697, USA
[1] catrakis@uci.edu, [2] raguirre@uci.edu, [3] jnathman@uci.edu, [4] garciap@uci.edu

ABSTRACT

Properties of turbulent fluid interfaces and regions are investigated experimentally and theoretically with applications to aero-optics and mixing. Two large-scale flow facilities enable the examination of refractive interfaces and diffusive interfaces in fully-developed gas-phase and liquid-phase turbulent separated shear layers and jets, i.e. at flow conditions above the mixing transition. The separated shear layer and the jet are key flow geometries, respectively, for practical problems in aero-optics and mixing. Basic relations are considered regarding the surface area of the interfaces, the volume of fluid regions bounded by the interfaces, and the physical interfacial thickness. These quantities have different sensitivities to large scales and small scales. Resolution-scale effects are also considered based on scale-local density functions corresponding to each quantity. For the aero-optically generated fields, the experimentally-derived large-scale contributions to the wavefront distortions are interpreted in terms of a physical model based on the regions bounded by high-gradient refractive interfaces. For the turbulent-mixing fields, the dynamical behavior of the volume of the region of mixed fluid exhibits strong robustness to resolution-scale effects. The present experimental database, physical-modeling approaches, and findings indicate that the large-scale properties of turbulent interfaces and regions can be directly examined and quantified at large Reynolds numbers.

1. INTRODUCTION

Knowledge of the behavior of turbulent fluid interfaces, as well as fluid regions bounded by interfaces, is useful in a variety of basic and applied problems as noted in review articles on turbulent flows and turbulence-influenced phenomena (Catrakis 2004, Jumper & Fitzgerald 2001, Sreenivasan 1999). This is because physical or chemical effects often occur across or on fluid interfaces, e.g. molecular diffusion, chemical reactions, electromagnetic-/optical-wave propagation, or acoustic-wave propagation. From a physical point of view, therefore, turbulent interfaces provide a useful basis for developing descriptions that can be related to practical quantities such as the aero-optical Strehl ratio or the turbulent mixing efficiency.

Examples of turbulent interfaces are diffusive or non-diffusive scalar interfaces which are typically associated with isosurfaces of the concentration, density, temperature, or refractive index (Sreenivasan 1991). Another example is the turbulent/nonturbulent interface which is the outer boundary between vortical vs. irrotational motion (Bisset *et al.* 2002). Examples of engineering applications and other problems sensitive to interfacial behavior include aero-optics, directed-energy propagation, film cooling, combustion, atmospheric dispersion, oceanic mixing.

Fundamentally, interfacial properties provide clues to the distribution of physical scales. At large Reynolds numbers, there is a wide distribution of scales and there are numerous open questions concerning the physical behavior or flow structure as a function of scale. For example, the vortical structure of turbulent flows at large scales and small scales remains unclear (Pullin & Saffman 1998) . The presence and extent of scale-independent or fractal behavior, at the small scales, is an open topic despite various efforts in this direction (Catrakis *et al.* 2002) . At the large scales, the behavior is most likely strongly scale dependent and is also an open topic despite the understanding that large organized structures are key elements of the structure depending on the flow conditions (Roshko 1976).

Depending on the application and the practical quantity of interest, large-scale or small-scale interfacial properties are needed for the development of physical models. Often, it is highly desirable to be able to quantify the relative contributions of the large scales vs. the small scales. In practice, in both flow-imaging experiments and flow-simulation experiments, it is also useful to be able to quantify the effects of coarse graining, i.e. the dependence on resolution scale especially at large Reynolds numbers. Because turbulent interfaces have highly-irregular geometrical structure, especially at large Reynolds numbers, significant challenges persist in their examination, modeling, and optimization.

2. THEORETICAL CONSIDERATIONS

We start by denoting any turbulence-generated scalar-valued field as $q(\mathbf{x}, t)$, e.g. the refractive-index field or concentration field. It is useful, physically and practically, to represent such a field in terms of the interfaces which correspond to the isosurfaces of the field, i.e.:

$$q(\mathbf{x}, t) \;=\; \text{const.}\,, \tag{1}$$

noting, however, that the interfaces have a physical finite thickness whereas the isosurfaces have zero thickness. To quantify the interfaces and the fluid regions bounded by the interfaces, three quantities are particularly useful. The first is the interfacial area:

$$A(q)\,. \tag{2}$$

The second is the volume of the regions of fluid bounded by interfaces:

$$V(q)\,, \tag{3}$$

The third is the mean interfacial thickness:

$$\overline{h}(q)\,. \tag{4}$$

The emphasis on these quantities is motivated by the interfacial interpretation of the probability density $p_q(q)$:

$$p_q(q) \;\equiv\; \frac{A(q)}{V_{\rm ref}}\,\overline{h}(q)\,, \tag{5}$$

where $V_{\rm ref}$ is the volume of a reference region in which $p_q(q)$ is normalized. The mean interfacial thickness $\overline{h}(q)$ is the average of the local interfacial thickness $h(q)$ along the interface. In general terms, the local interfacial thickness per unit q can be represented in terms of the inverse of the magnitude $|\nabla q|$ of the local gradient across the interface, i.e.

$$h(q) \;\equiv\; |\nabla q(\mathbf{x},t)|^{-1} \;=\; \left|\frac{\partial q}{\partial n}\right|^{-1}\,. \tag{6}$$

It is geometrically evident that the fluid-interface area $A(q)$ and the fluid-region volume $V(q)$ are directly related as:

$$V(q) \;=\; \int_q^{q_{\rm max}} A(q')\,\overline{h}(q')\,{\rm d}q'\,. \tag{7}$$

Conversely,

$$A(q) \;=\; \frac{1}{\overline{h}(q)}\,\left|\frac{{\rm d}V(q)}{{\rm d}q}\right|\,. \tag{8}$$

The two preceding relations suggest that the interfacial area can be expected to be highly sensitive to the small scales whereas the fluid-region volume can be expected to be dominated by the large scales.

In practice, it is also helpful to consider resolution-scale effects with coarse-grained quantities $A(q;\lambda)$, $V(q;\lambda)$, and $\overline{h}(q;\lambda)$, where λ is the resolution scale, i.e. retaining fluid-interface/-region information at scales from the resolution scale λ to the largest scale L. Thus, the coarse-grained interfacial area can be expressed as:

$$A(q;\lambda) \;=\; \int_\lambda^L g_A(q;\lambda')\,{\rm d}\lambda'\,, \tag{9}$$

where $g_A(q;\lambda)$ is the scale-local area density. The coarse-grained region volume can be expressed as:

$$V(q;\lambda) \;=\; \int_\lambda^L g_V(q;\lambda')\,{\rm d}\lambda'\,, \tag{10}$$

where $g_V(q;\lambda)$ is the scale-local volume density. The coarse-grained interfacial thickness can be expressed as:

$$\overline{h}(q;\lambda) \;=\; \int_\lambda^L g_h(q;\lambda')\,{\rm d}\lambda'\,, \tag{11}$$

where $g_h(q;\lambda)$ is the scale-local thickness density.

The significance and utility of scale-local measures, and their relation to scale-cumulative quantities, has been demonstrated in the context of the area-volume ratio in previous work (Catrakis *et al.* 2002) The above scale-local densities provide a means to quantify and compare the large-scale vs. small-scale contributions to the properties of fluid interfaces and fluid regions. Furthermore, knowledge of the small-scale behavior of these scale-local densities is useful for resolution-scale scaling in large-eddy simulations or finite-resolution flow imaging (Meneveau & Katz 2000, Clemens 2002). .

3. FLOW FACILITIES, CONDITIONS, AND IMAGING

Two relatively-large-scale flow facilities have been developed at UCI, as shown in figures 1 and 2, which enable the examination of gas-phase and liquid-phase turbulent flows. The variable-pressure flow facility in figure 1 is especially useful for aero-optics studies. The octagonal tank in figure 2 is suited for studies of turbulent mixing. Together, these two facilities can generate flows spanning four decades in Reynolds number, i.e.

$$10^4 \;\lesssim\; Re \;=\; \frac{\rho\,U\,L}{\mu} \;\lesssim 10^8\,, \tag{12}$$

with a Mach-number range of:

$$0.3 \;\lesssim\; M \;=\; \frac{U}{a} \;\lesssim 2.5\,. \tag{13}$$

The capability to probe gases as well as liquids provides a span of four decades in Schmidt number, i.e.

$$1 \;\lesssim\; Sc \;=\; \frac{\nu}{\mathcal{D}} \;\lesssim 10^4\,. \tag{14}$$

The aero-optics vessel provides elevated pressures up to $p \simeq 20\,{\rm atm}$. Combined with laser and optical diagnostics, these facilities produce high-resolution imaging measurements of turbulent interfaces in aero-optics and mixing. Quantitative flow images, as shown in figures 3 and 5, are recorded using laser-induced fluorescence techniques in air and in water by molecular seeding with acetone vapor and disodium fluorescein, respectively. For the aero-optics and mixing studies, the two flow geometries examined are the separated shear layer and the jet, respectively.

4. APPLICATIONS TO AERO-OPTICAL INTERACTIONS

In aero-optics, in order to contribute to the development of physical models of optical beam propagation through variable index-of-refraction turbulent flows, it is helpful to consider the role of the refractive fluid interfaces. These correspond to the refractive-index (scalar) isosurfaces:

$$n\,(\mathbf{x},t) \;=\; {\rm const.} \tag{15}$$

but in addition one must take into account the physical thickness of the interfaces in a manner similar to the approach described above in section 2.

There are several reasons why it is helpful to relate the turbulence-distorted optical wavefronts to the turbulence-generated refractive fluid interfaces. Firstly, the actual aero-optical interactions such as wavefront refraction take place physically across these interfaces. Secondly, especially at large Reynolds numbers, there is evidence that the dominant contributions to the optical-wavefront distortions arise primarily from the unsteady outer interfaces for the case of low-compressibility dissimilar-gas shear layers (Dimotakis *et al.* 2001). In other words, the spatial extent and shape of the turbulent regions:

$$n_1 \;\lesssim\; n\,(\mathbf{x},t) \;\lesssim\; n_2\,, \tag{16}$$

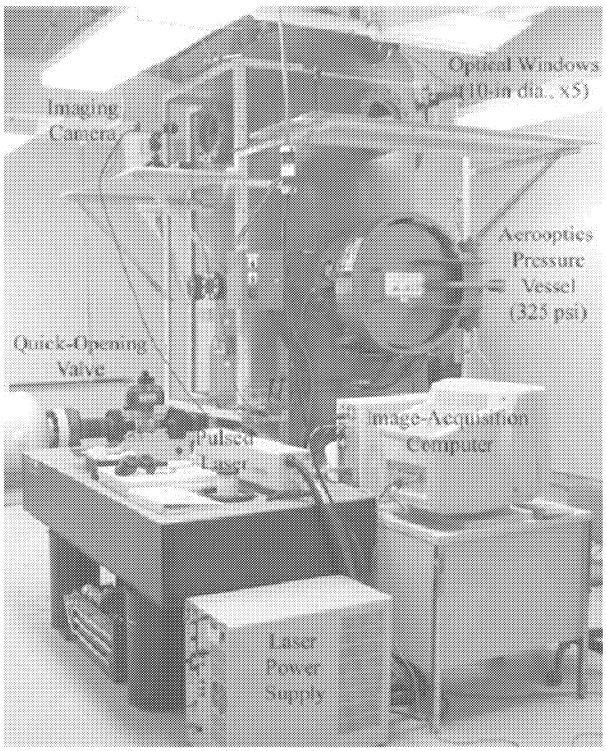

Figure 1: Photograph of the Aero-Optics Variable-Pressure Flow Facility at UC Irvine.

Figure 2: Photograph of the Octagonal-Tank Atmospheric-Pressure Flow Facility at UC Irvine.

is a key element in order to capture the dominant optical-phase distortions. More generally, the dominant interfaces need not be only the outer interfaces. For example, highly three-dimensional flows most likely will require modeling in terms of both outer and internal interfaces. Also, high-compressibility flows will require representation in terms of outer as well as internal interfaces. The planar two-dimensional low-compressibility shear layer is, in a sense, a restrictive flow-geometry example but it does illustrate convincingly that the outer interfaces are sufficient to model the dominant aero-optical interactions. This is because the organized large-scale structures result in large-scale homogeneity of the refractive-index field for the above-mentioned shear layer (Brown & Roshko 1974). For a more complete understanding, one would have to also understand the relation between the refractive interfaces and the vortical structure of the flow.

A key quantity in the study of aero-optics, and particularly useful for aero-optical optimization of directed-energy systems, is a beam attenuation measure known as the Strehl ratio S. The Strehl ratio is the peak propagated intensity of the beam normalized by the distortion-free diffraction-limited peak intensity:

$$S \equiv \frac{I_{\text{peak}}}{I_{\text{peak},0}} . \tag{17}$$

It can be shown that the Strehl ratio is directly determined by the optical path difference (OPD) in the so-called large-aperture approximation. In general, the OPD will depend on the Reynolds number Re, Mach number M, and flow geometry:

$$\text{OPD} \equiv \text{OPD}\,(Re, M, \text{flow geometry}) . \tag{18}$$

Aero-optical optimization, in most applications, entails determining the flow conditions and flow geometry that minimize the wavefront distortions. In order to do this, it would be useful to be able to identify and modify the dominant interfaces, i.e. the interfaces which produce the primary wavefront distortions. It should be noted that one can expect a direct relation between the optical-wavefront structure and the refractive-interface structure. The optical wavefronts can be represented physically as the isosurfaces of the optical path length (OPL), i.e.,

$$\text{OPL}\,(\mathbf{x}, t) = \text{const.} \tag{19}$$

Because the optical path length is an integral over the refractive interfaces however, knowledge of the OPL or related integrated quantities of the refractive-index field is not sufficient to uniquely relate the flow structure to the wavefront structure. For this reason, in the context of experiments, it is essential to be able to record the refractive-index field directly. An example is shown in figure 1 where acetone-vapor fluorescence was utilized to record the refractive-index field in a purely-gaseous separated shear layer.

A large reduction in interfacial information, for the separated shear layer, is possible in terms of capturing the dominant aero-optical distortions based on the high-gradient interfaces using the interfacial-fluid-thickness (IFT) approach developed previously (Catrakis 2004). The basic idea is to retain the location of the high-gradient interfaces and also the thickness variations along these interfaces, at a finite resolution in practice. Then, the dominant large-scale contributions to the OPL can be captured effectively in terms of the modeled interfaces as:

$$[\text{OPL}(\mathbf{x}, t)]_{\text{dominant}} \simeq \int_{\text{ray}} n^*(\ell, t)\; h_{n^*,\ell}\; |\mathrm{d}n^*| , \tag{20}$$

Figure 3: Experimental quantitative image of a gas-phase turbulent separated shear layer at $Re \sim 10^6$, $M \sim 0.9$, and $Sc \sim 1$, at a pressure of $\sim 3\,\mathrm{atm}$, recorded in the UC Irvine Aero-Optics Flow Facility.

where $h_{n^*,\ell} = 1/|\nabla n^*|_\ell$ is the effective interfacial thickness, i.e. the component along the local optical-ray direction, and ℓ is the propagation distance. The starred quantities denote the modeled refractive-index with reduced interfacial information.

An example of the effectiveness in capturing the large-scale aero-optical distortions is shown in figure 4 for the separated weakly-compressible shear layer, where the dashed curve corresponds to retaining only large-scale low-gradient regions bounded by high-gradient interfaces. The reduction in interfacial information can be expected to be utilized in developing adaptive-optic systems with active flow control, by reducing the bandwidth or resolution required to dynamically track and compensate for the dominant optical distortions.

5. APPLICATIONS TO TURBULENT MIXING EFFICIENCY

In mixing, a useful quantity is the volume fraction α_m of mixed fluid which in general depends as:

$$\alpha_\mathrm{m} \;\equiv\; \alpha_\mathrm{m}\,(Re, M, Sc, \text{flow geometry})\;. \tag{21}$$

It is a mixing-efficiency measure given by the concentration field $c(\mathbf{x}, t)$ and probability density $p_c(c)$:

$$\alpha_\mathrm{m} = \int_{\mathcal{M}} p_c(c)\;\mathrm{d}c = \int_{\mathcal{M}} \frac{A(c)}{V_\mathrm{ref}}\;\overline{h}_c(c)\;\mathrm{d}c\,, \tag{22}$$

where $\mathcal{M}$ is the mixed-fluid region. One of the frequently-used definitions of the mixing efficiency (e.g. King *et al.* 1999) is

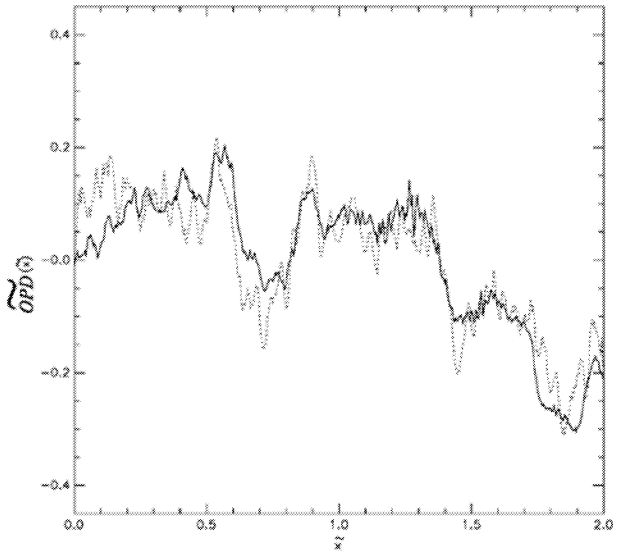

Figure 4: Spatial profiles of the wavefront optical path difference (OPD) for gas-phase separated shear layers as in figure 3. Experimental data (solid curve) vs. interfacial model (dashed curve).

the mixed-fluid volume fraction or mixture fraction. It is helpful, in practice, to first identify the outer interface separating mixed fluid from pure fluid as demonstrated in recent work (Catrakis *et al.* 2002).

In principle, in order to examine the mixing efficiency in terms of interfacial properties, it would seem that knowledge of the area $A(c)$ over all internal and outer interfaces is needed as well as of the mean thickness $\overline{h}(c)$ of each interface:

$$\overline{h}(c) \;=\; \left\langle \left|\frac{\partial c}{\partial s}\right|^{-1} \right\rangle_c \;=\; \frac{1}{A(c)} \int\!\!\int_{S_c} \left|\frac{\partial c}{\partial s}\right|^{-1} \mathrm{d}S_c\,, \tag{23}$$

where S_c denotes the surface of the interface over which the mean interfacial thickness is evaluated. A potential difficulty, however, is that the surface area $A(c)$ is highly sensitive to the small scales. This is evident theoretically by realizing that the surface area is a derivative of the volume, i.e.:

$$A(c) \;=\; \frac{1}{\overline{h}(c)}\;\frac{|\mathrm{d}V(c)|}{\mathrm{d}c}\,. \tag{24}$$

Experimental and numerical studies, for example, have shown that the surface area of turbulent interfaces is actually dominated by the small scales (Bisset *et al.* 2002). The mean interfacial thickness is also sensitive to the small scales since it is a gradient-based quantity and also because of the intermittency of turbulent mixing. Thus, modeling and descriptions of the mixing efficiency using a surface-based approach are possible in principle but are known to be highly sensitive to resolution limitations.

An alternative approach, which we term the volume-based approach, is directly based on the volume V_mixed of the mixed-fluid region bounded by the outer interfaces. This volume can be expected to be dominated by the large scales, i.e. to be weakly sensitive to the small scales, especially above the mixing transition. This is because of the strong large-scale vorticity/concentration correlations that occur above the transition, as opposed to below the transition, as indicated by recent

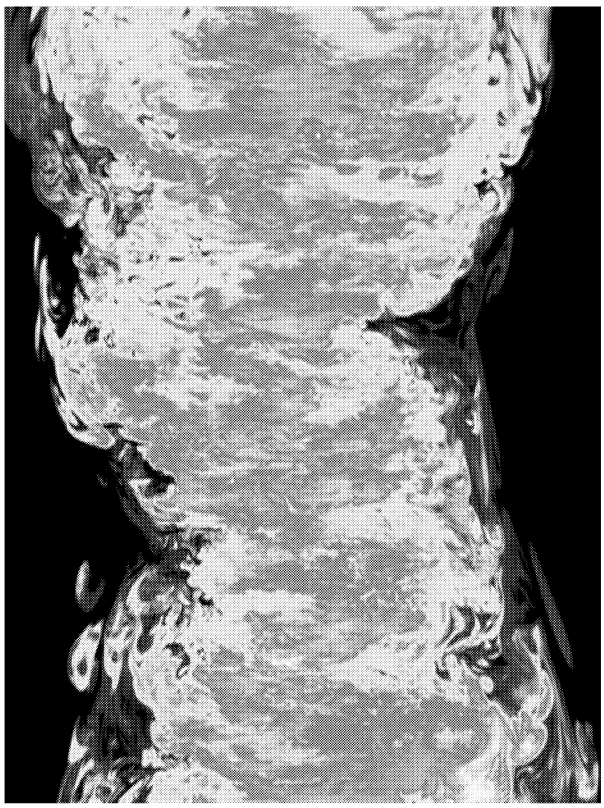

Figure 5: Experimental quantitative image of a liquid-phase turbulent jet at $Re \sim 10^4$ and $Sc \sim 10^3$, with time increasing to the right, recorded in the UCI Octagonal-Tank Flow Facility.

work (Catrakis *et al.* 2002). . Furthermore, the volume-based approach does not require knowledge of the concentration-threshold dependence, since it only requires outer-interface information. The weak sensitivity of the volume to the small-scale interfacial features can also be appreciated by expressing the volume of the mixed-fluid region as an integral of the surface area of the internal and outer interfaces:

$$V_{\mathrm{mixed}} \;=\; \int_{\mathrm{mixed}} A(c)\;\overline{h}(c)\;\mathrm{d}c\,, \qquad (25)$$

cf. equation 24. Thus, in contrast to the surface-based approach, one can anticipate robustness to resolution-scale effects by using the volume-based approach.

In the volume-based approach, the mixed-fluid region is identified first as the complement of the pure-fluid region. The volume in three dimensions, or area in two dimensions, of the mixed-fluid region is subsequently evaluated. For the present flow conditions, the ensemble-averaged value of the mixing efficiency was evaluated at full resolution and is:

$$\alpha_{\mathrm{m}} \;\simeq\; 60.7\%\,, \qquad (26)$$

with an uncertainty estimated at $\pm 0.05\%$. This mixing-efficiency value corresponds to the jet flow geometry and the present flow conditions. One can expect a dependence on both Reynolds number and Schmidt number, as well as flow geometry, in general.

To examine resolution-scale effects, the concentration field was coarse grained first and the interfaces were identified

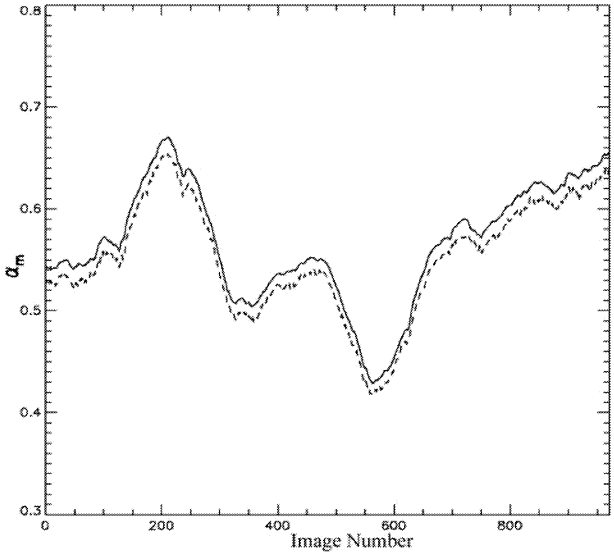

Figure 6: Dynamical behavior of the mixing efficiency, as a volume fraction of mixed fluid, for liquid-phase jets as in figure 5. Full-resolution (solid curve) vs. coarse-grained (dashed curve) experimental data.

subsequently from the coarse-grained field. For the coarse graining, a resolution scale of $\lambda/L = 1/10$, normalized by the large scale L, was chosen. The coarse graining was performed on the three-dimensional space–time concentration fields. As shown in figure 6, the large-scale dynamical behavior is captured with less than $\sim 2\%$ difference even with coarse-grained data at a 100-fold reduction in flow information. This indicates robustness to resolution effects for the mixed-fluid volume fraction.The ensemble-averaged volume of the coarse-grained mixed-fluid region was evaluated, resulting in a mixing-efficiency value of:

$$[\alpha_{\mathrm{m}}]_{\mathrm{coarse}} \;\simeq\; 59.5\%\,, \qquad (27)$$

with an estimated uncertainty also of $\pm 0.05\%$, cf. equation 26. In other words, there is less than 2% difference for a ten-fold resolution change, per dimension, in the volume V_{mixed} of the identified mixed-fluid region and therefore of the evaluated mixing efficiency α_{m}, between the full-resolution and coarse-grained interfacial information. In contrast to the low sensitivity of the mixed-fluid region volume V_{mixed} and the mixing efficiency α_{m}, there is high sensitivity to the small scales for the interfacial surface area $A(c)$, the mean interfacial thickness $\overline{h}(c)$, or the probability density $p(c)$.

CONCLUSIONS

The present results on interfacial behavior in fully-developed turbulent flows have emphasized properties that are useful to quantify the dependence of the flow structure on scale including resolution-scale dependence, the limiting flow behavior at large Reynolds numbers or at high compressibilities, and the extent to which the dominant effects of the interfaces can be optimized. These ideas have immediate implications in aero-optics and mixing.

In aero-optics, the experimentally-derived large-scale wavefront distortions are physically modeled based on the regions bounded by high-gradient refractive interfaces. The role of refractive interfaces in large-scale aero-optical interactions can

be directly examined, at finite resolution, in high-Reynolds-number single-stream compressible shear layers generated in the UC Irvine variable-pressure flow facility. The Reynolds number based on the visual thickness is $Re \sim 6 \times 10^6$ and the convective Mach number is $M_c \sim 0.4$. The high-gradient boundaries are found to be primarily responsible for the large-scale aero-optical interactions. Specifically, a physical model utilizing these high-gradient boundaries is able to reproduce well the large-scale optical-wavefront distortions. The present findings correspond to the effects of mixing between the freestream and ambient gases, and are useful for comparisons to other effects such as density effects. The reduction in interfacial information has implications for developing adaptive-optics techniques with active flow control, by facilitating the development of methods to reduce the bandwidth or resolution required to dynamically track and compensate for the dominant optical distortions.

In turbulent mixing, the dynamical behavior of the volume of the mixed-fluid region exhibits strong robustness to resolution-scale effects. The present finding of less than 2% difference in the mixing efficiency for a tenfold reduction in resolution scale, for each dimension, corresponds therefore to $1,000$ times less concentration-field information for three-dimensional data. This is a major savings in the interfacial information needed to account for the dominant behavior of the mixing efficiency. This behavior can be expected, therefore, at larger Reynolds numbers and has thus practical implications in the context of physical modeling, prediction, and optimization of the mixing efficiency. In large-eddy simulations (LES), for example, the robustness to small scales has two implications regarding sub-grid scale modeling for the mixture fraction. The limiting behavior of the mixing efficiency can be physically modelled in terms of the large-scale outer interfaces and will be strongly dependent on the flow geometry. For flow optimization, this indicates that modification of the large-scale features of the outer interfaces can be effective in enhancing, or reducing, the mixing efficiency.

There are broader implications of the present results with regard to the following general questions in turbulence. How does the interfacial behavior depend on scale? What is the limiting interfacial behavior, e.g. at large Reynolds numbers? What are the prospects for interfacial optimization and regularization? Regarding the dependence of the flow behavior on scale, the present results indicate in conjunction with earlier results (e.g. Catrakis *et al.* 2002) that the energy-containing range of scales is strongly scale dependent. Thus, the methods previously developed that generalize fractal concepts to scale-dependent behavior (e.g. Catrakis 2004) can be expected to be directly applicable to quantifying the upper range of interfacial scales. This is helpful practically in order to quantify the relative contributions of the large vs. small scales in a wide variety of applications, including aero-optics and mixing. Regarding the limiting behavior of fluid interfaces or fluid regions, for example at large Reynolds numbers, the present results suggest a means to develop physical models that can capture the large-Reynolds-number behavior in terms of the large or small scale contributions which are dominant depending on the physical quantity in question, e.g. the large scales dominate the volume of fluid regions whereas the small scales dominate the surface area of fluid interfaces. Regarding optimization and regularization of interfaces and regions, the present results indicate new prospects for optimizing and regularizing time-dependent flow quantities that are dominated by large scales. The strong scale dependence of the energy-containing range of interfacial scales provides an ingredient that can be examined, modeled, and modified according to the basic or applied objective of interest in both optimization and regularization.

ACKNOWLEDGEMENTS

We are grateful for the support of the Air Force Office of Scientific Research (Dr. J. Schmisseur and Dr. T. Beutner), the Defense University Research Instrumentation Program, the Henry Samueli School of Engineering, as well as the National Science Foundation (Prof. J. Foss) which has enabled the initiation of new basic and applied studies of turbulence through a National Science Foundation Career Award.

REFERENCES

D. K. Bisset, J. C. Hunt, and M. M. Rogers. The turbulent/non-turbulent interface bounding a far wake. *J. Fluid Mech.*, 451:381–410, 2002.

G. L. Brown and A. Roshko. On density effects and large scale structure in turbulent mixing layers. *J. Fluid Mech.*, 64:775–816, 1974.

H. J. Catrakis. Turbulence and the dynamics of fluid interfaces with applications to mixing and aero-optics. In N. Ashgriz and R. Anthony, editors, *Recent Research Developments in Fluid Dynamics*, volume 5, pages 115–158. Transworld Research Network Publishers, Kerala, India, 2004.

H. J. Catrakis and R. C. Aguirre. New interfacial fluid thickness approach in aero-optics with applications to compressible turbulence. *AIAA J.*, 42(10):1973–1981, 2004.

H. J. Catrakis, R. C. Aguirre, and J. Ruiz-Plancarte. Area–volume properties of fluid interfaces in turbulence: scale-local self-similarity and cumulative scale dependence. *J. Fluid Mech.*, 462:245–254, 2002.

H. J. Catrakis, R. C. Aguirre, J. Ruiz-Plancarte, R. D. Thayne, B. A. McDonald, and J. W. Hearn. Large-scale dynamics in turbulent mixing and the three-dimensional space-time behaviour of outer fluid interfaces. *J. Fluid Mech.*, 471:381–408, 2002.

N. T. Clemens. Flow imaging. In *Encyclopedia of Imaging Science and Technology*, pages 390–419. Wiley, 2002.

P. E. Dimotakis, H. J. Catrakis, and D. C. L. Fourguette. Flow structure and optical beam propagation in high-Reynolds-number gas-phase shear layers and jets. *J. Fluid Mech.*, 433:105–134, 2001.

E. J. Jumper and E. J. Fitzgerald. Recent advances in aero-optics. *Prog. Aerospace Sci.*, 37:299–339, 2001.

G. F. King, J. C. Dutton, and R. P. Lucht. Instantaneous, quantitative measurements of molecular mixing in the axisymmetric jet near field. *Phys. Fluids*, 11:403–416, 1999.

C. Meneveau and J. Katz. Scale-invariance and turbulence models for large-eddy simulation. *Annu. Rev. Fluid. Mech.*, 32:1–32, 2000.

D. I. Pullin and P. G. Saffman. Vortex dynamics in turbulence. *Annu. Rev. Fluid. Mech.*, 30:31–51, 1998.

A. Roshko. Structure of turbulent shear flows: a new look. *AIAA J.*, 14:1349–1357, 1976.

K. R. Sreenivasan. Fractals and multifractals in fluid turbulence. *Annu. Rev. Fluid. Mech.*, 23:539–600, 1991.

K. R. Sreenivasan. Fluid turbulence. *Rev. Mod. Phys.*, 71:S383–S395, 1999.